Analysis and design of photovoltaic three-phase grid-connected inverter using passivity-based control

Zainab Mahmood Abed, Turki Kahawish Hassan, Kassim Rasheed Hameed
Department of Electrical Engineering, College of Engineering, Mustansiriyah University, Baghdad, Iraq

Article Info	ABSTRACT
  	This paper presents photovoltaic three-phase grid-connected inverter with an inductor-capacitor-inductor (LCL)-filter. For robustness against variation of filter parameters and external disturbance, the passivity-based control (PBC) method has been adopted. In this method, there are two interactively coupled feedforward terms and three damping gains in the control loops which are designed to limit the steady state error of grid current. Boost converter with P&O maximum power point tracker (MPPT) is used for each photovoltaic (PV) string to extract maximum power and to raise the PV voltage to a value suitable for the grid-connected inverter. The outputs of all boost converters are connected in parallel and controlled to fixed reference voltage using proportional-integral (PI) controller to make the direct-current (DC) link voltage robust against variations in sun radiation intensity and system parameters change. The suggested system is analyzed, designed and simulated using PSIM program. 1 kW, 2 kW, and 3 kW PV systems connected to grid of 220 V/50 Hz are tested and the results show the validity of the suggested grid-connected PV systems and robustness against filter parameters variation.

Corresponding Author:

Zainab Mahmood Abed
Electrical engineering department, college of engineering, Mustansiriyah university
Baghdad, Iraq
Email: zenababed@uomustansiriyah.edu.iq

1. INTRODUCTION

Nowadays, the renewable energy and relative technologies have been significant attention. The more important link between the renewable energy and grid is the grid connected inverter (GCI) with suitable filter to reduce the current harmonics, such as inductor (L), inductor-capacitor (LC), and inductor-capacitor-inductor (LCL) filters. The LCL filter has better performance of harmonic attenuation and lower cost compared with other types [1]–[3]. To enhance the performance of GCI with filter, many control strategies are used such as proportional resonance (PR) [4] and proportional integral (PI) controllers with passive damping method [5], [6], active damping method [7]–[10] and hybrid damping method [11], [12]. The damping methods are used to enhance the performance of PR and PI controllers by reduction the resonance effect, in another hand, these methods add extra cost like extra power in passive damping method and extra number of sensors in active damping method. Another non-linear methods are used to enhance the performance of GCI with filter, such as predictive control [13], [14], deadbeat control [15], [16] slide model control [17], [18], adaptive control [19], [20], and passivity based control with wind system [21], railway systems [22], [23], energy storage systems [24], [25], islanded AC microgrid [26] and GCI systems [27]–[34]. The passivity-based control (PBC) strategy has simple modeling process and better performance against parameters variations with different types of filters.

The GCI system is coupled with L filter [27], [28] and LC filter [29], [30] where the discrete root locus with unit step response and traditional analysis method like PI parameters design are used, there is one feedforward in control loop and one damping gain of PBC controller which is selected depending on attenuation of delay influence on the inverter, the feedforward term has no effect on stability of the system so it can be neglected. The GCI system is also coupled with the LCL filter [31]−[34] where there are two feedforwards in control loop and three damping gains, the GCI system is used with fixed DC supply voltage. In this paper a PV system (demonstrated in section III-B) is used to supply grid through GCI with LCL filter and PBC strategy is used as shown in Figure 1, where the additional DC voltage loop is used to enhance the performance of GCI system.
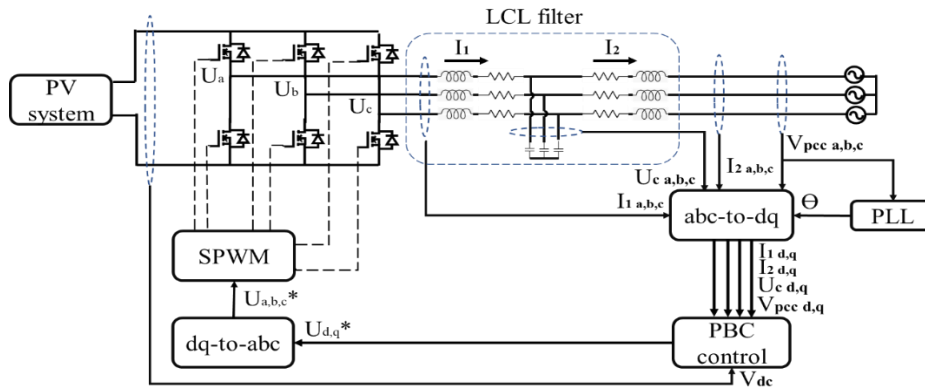

Figure 1. Implementation of proposed system

The rest of this paper is organized as follows: the description of proposed system and mathematical model of LCL filter and PBC controller are introduced in section 2. Design of proposed system is presented in section 3. Many tests of changes in light intensity, filter parameters, and grid voltage are applied to check the robustness of the proposed system in section 4, and the conclusion is summaries in section 5.

2.   MATHEMATICAL MODELING OF LCL FILTERED THREE PHASE GCI WITH PBC
2.1. The mathematical model of LCL filtered system
The mathematical model of LCL filtered system is:

$$L_1 \frac{di_{1k}}{dt} + R_1 i_{1k} + u_{ck} = u_k$$
$$C \frac{du_{ck}}{dt} + i_{2k} - i_{1k} = 0 \tag{1}$$
$$L_2 \frac{di_{2k}}{dt} + R_2 i_{2k} - u_{ck} = -v_{pcck}$$

Where; L_1 is the inverter side inductance, R_1 is inverter side parasitic resistance, u_c is capacitance voltage, u is inverter voltage, C is filter capacitance, L_2 is grid side inductance, R_2 is grid side parasitic resistance, i_1 is inverter current, i_2 is grid current, v_{pcc} is grid voltage, and k=a,b,c.
To get better control performance, abc-to-dq transformation is applied to (1), the new model is:

$$L_1 \frac{di_{1d}}{dt} + R_1 i_{1d} + \omega L_1 i_{1q} + u_{cd} = u_d$$
$$L_1 \frac{di_{1q}}{dt} + R_1 i_{1q} - \omega L_1 i_{1d} + u_{cq} = u_q$$
$$C \frac{du_{cd}}{dt} + i_{2d} + \omega C u_{cq} - i_{1d} = 0$$
$$C \frac{du_{cq}}{dt} + i_{2q} - \omega C u_{cd} - i_{1q} = 0 \tag{2}$$
$$L_2 \frac{di_{2d}}{dt} + R_2 i_{2d} + \omega L_2 i_{2q} - u_{cd} = -v_{pccd}$$
$$L_2 \frac{di_{2q}}{dt} + R_2 i_{2q} - \omega L_2 i_{2d} - u_{cq} = -v_{pccq}$$

The Euler Lagrange model is used to describe the system for simplify analysis. The state variables are defined as x=$(i_{1d}\ i_{1q}\ u_{cd}\ u_{cq}\ i_{2d}\ i_{2q})^T$ and (2) is rewritten as:

$$A\dot{x} + Bx + Cx = u \tag{3}$$

Where;

$$A = \begin{bmatrix} L_1 & 0 & 0 & 0 & 0 & 0 \\ 0 & L_1 & 0 & 0 & 0 & 0 \\ 0 & 0 & C & 0 & 0 & 0 \\ 0 & 0 & 0 & C & 0 & 0 \\ 0 & 0 & 0 & 0 & L_2 & 0 \\ 0 & 0 & 0 & 0 & 0 & L_2 \end{bmatrix}$$

$$B = \begin{bmatrix} 0 & -\omega L_1 & 1 & 0 & 0 & 0 \\ \omega L_1 & 0 & 0 & 1 & 0 & 0 \\ -1 & 0 & 0 & -\omega C & 1 & 0 \\ 0 & -1 & \omega C & 0 & 0 & 1 \\ 0 & 0 & -1 & 0 & 0 & -\omega L_2 \\ 0 & 0 & 0 & -1 & \omega L_2 & 0 \end{bmatrix}$$

$$C = \begin{bmatrix} R_1 & 0 & 0 & 0 & 0 & 0 \\ 0 & R_1 & 0 & 0 & 0 & 0 \\ 0 & 0 & 0 & 0 & 0 & 0 \\ 0 & 0 & 0 & 0 & 0 & 0 \\ 0 & 0 & 0 & 0 & R_2 & 0 \\ 0 & 0 & 0 & 0 & 0 & R_2 \end{bmatrix}$$

And $u = [u_d \quad u_q \quad 0 \quad 0 \quad -v_{pccd} \quad -v_{pccq}]^T$ According to the theory of passivity, the LCL filtered system is strictly passive, and the controller can be designed by applying PBC [33].

2.2. PBC control

The reference state variables are defined as:

$$x^* = [i_{1d}{}^* \quad i_{1q}{}^* \quad u_{cd}{}^* \quad u_{cq}{}^* \quad i_{2d}{}^* \quad i_{2q}{}^*]^T \tag{4}$$

While the error vector is defined as $x_e = x^* - x$, the Euler Lagrange equation can be rewritten as:

$$A(\dot{x}^* - \dot{x}_e) + B(x^* - x_e) + C(x^* - x_e) = u$$

$$A\dot{x}_e + Bx_e + Cx_e = A\dot{x}^* + Bx^* + Cx^* - u \tag{5}$$

To accelerate the convergence speed, a damping matrix k_d is added to error system, where:

$$k_d = diag\{k_2 \quad k_2 \quad k_1 \quad k_1 \quad k_0 \quad k_0\} \tag{6}$$

Where; k_1, $k_2 > 0$ and k_0 can be replaced by PI controller to enhance the steady state response. Substitution (6) into (5) to get:

$$A\dot{x}_e + Bx_e + Cx_e + k_d x_e = A\dot{x}^* + Bx^* + Cx^* + k_d x_e - u \tag{7}$$

If x_e is zero, the left side of (7) is zero too, the control law can be written in details as:

$$\left. \begin{aligned} &L_1 \frac{di_{1d}{}^*}{dt} + R_1 i_{1d}{}^* + \omega L_1 i_{1q}{}^* + k_2(i_{1d}{}^* - i_{1d}) + u_{cd}{}^* = u_d \\ &L_1 \frac{di_{1q}{}^*}{dt} + R_1 i_{1q}{}^* - \omega L_1 i_{1d}{}^* + k_2(i_{1q}{}^* - i_{1q}) + u_{cq}{}^* = u_q \\ &C \frac{du_{cd}{}^*}{dt} + \omega C u_{cq}{}^* + k_1(u_{cd}{}^* - u_{cd}) + i_{2d}{}^* - i_{1d}{}^* = 0 \\ &C \frac{du_{cq}{}^*}{dt} - \omega C u_{cd}{}^* + k_1(u_{cq}{}^* - u_{cq}) + i_{2q}{}^* - i_{1d}{}^* = 0 \\ &L_2 \frac{di_{2d}{}^*}{dt} + R_2 i_{2d}{}^* + \omega L_2 i_{2q}{}^* + k_0(i_{2d}{}^* - i_{2d}) - u_{cd}{}^* = -v_{pccd} \\ &L_2 \frac{di_{2q}{}^*}{dt} + R_2 i_{2q}{}^* - \omega L_2 i_{2d}{}^* + k_0(i_{2q}{}^* - i_{2q}) - u_{cq}{}^* = -v_{pccq} \end{aligned} \right\} \tag{8}$$

$$I_{2q}{}^* = k_{p_v}(V_{ref} - V_{dc}) + \int k_{i_v}(V_{ref} - V_{dc}) \tag{9}$$

Where V_{dc} is the inverter DC-link voltage, V_{ref} is the reference voltage and k_{pv}, k_{iv} are the proportional integral gains. The diagram of equivalent system using PBC with inverter DC-link voltage control in (8) and (9) is implemented as shown in Figure 2.
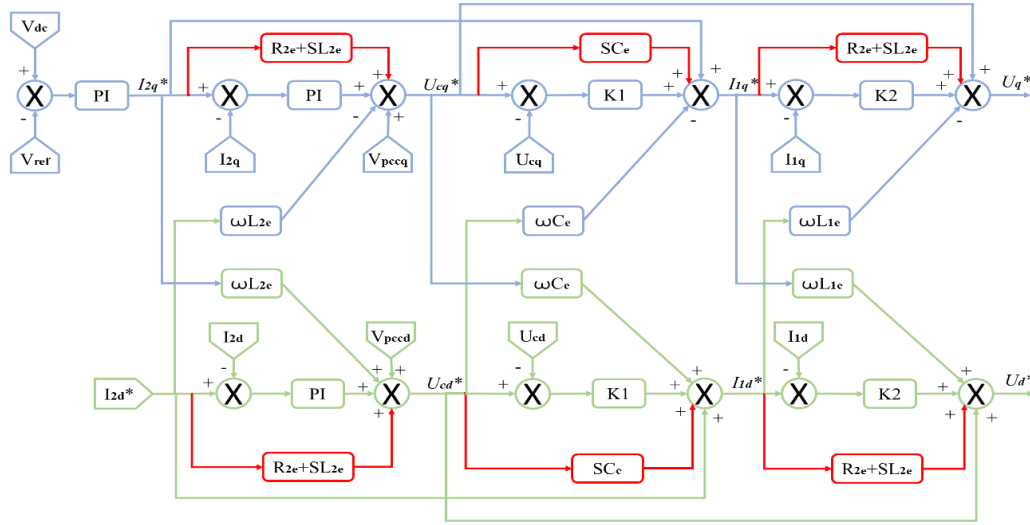

Figure 2. Implementation of PBC and inverter DC-link voltage control

The damping gains k_1 and k_2 can be calculated as explained in [33] by:

$$k_1 = \frac{C}{3T_s} \tag{10}$$

$$k_2 = \frac{L_1}{6\zeta^2 T_s} \tag{11}$$

where; C is the filter capacitance, L_1 is the inverter side inductance, T_s is the switching frequency, and ζ is the damping ratio which is $\frac{1}{\sqrt{2}}$ [33].

3. PROPOSED SYSTEM DESIGN
3.1. LCL filter

The power conversion of PV system (boost converter) and inverter injects harmonics into grid which affect the system operation and reduce the overall power factor. LCL filter is used in the proposed system to eliminate the harmonics effect [35]. The LCL filter is shown in Figure 3, and the limits of it is parameters can be calculated by (12).

$$L_1 \leq \frac{V_{DC}}{6F_{sw}\Delta I_{1\,max}} \tag{12}$$

Where; L_1 is the inverter side inductance, V_{DC} is the boosted DC voltage, $\Delta I_{1\,max}$ is the maximum inverter current ripple which is approximately 20% of grid current, and F_{sw} is the switching frequency [36].

$$C \leq 0.05 * \frac{I_2}{2\pi F_{ac}V_{ac}} \tag{13}$$

Where; C is the filter capacitance, I_2 is the grid current, V_{ac} is the grid voltage, and F_{ac} is the grid frequency.

$$L_2 = rL_1, r \leq 1 \tag{14}$$

Where; L_2 is the grid side inductance [37]. A grid inductance L_g is added to L_2 and it's value is uncertain, so it is choice practically [38]. According to (12), (13), and (14) the limits of LCL filter parameters in this paper are $L_1 \leq 10$ mH, $C \leq 4.34$ μF, $L_2 \leq 10$ mH.
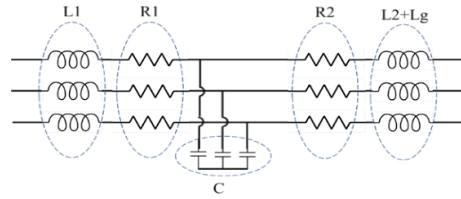
Figure 3. LCL filter design

3.2. PV system

A PV string of PSIM library consisting of 4 series connected PV panels, it is generated 1000 W of power at 1000 W/m² of light intensity. The PV system contains many of PV strings connected in parallel (through boost converter with MPPT for each string) according to the required power, many changes are occurred to the PV system to check the robust of the proposed system of this paper, firstly, the PV system works with different number of PV strings, secondly, the PV system works with different values of light intensity. The low output voltage of PV string is boosted to grid conjunction, a DC-to-DC converter is necessary to use between the PV string and the inverter [35]. in this paper a boost converter with maximum power point tracker (MPPT) is used and the output voltage of boost converter for each string is regulated to 720 V using PI controller. The PV system consisting of PV string and DC-to-DC boost converter is shown in Figure 4. The PV system provides DC power, a DC-to-AC inverter is used to convert the DC power to three phase AC power to supply the grid. The sinusoidal pulse width modulation (SPWM) method is used to control the switches of inverter with carrier frequency of 10000 Hz.
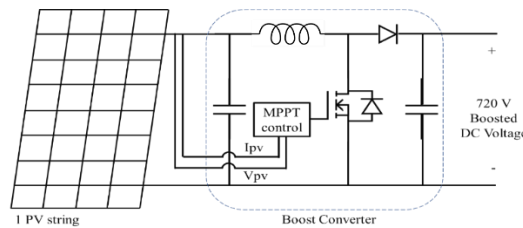

Figure 4. PV system with one PV string

4. RESULTS

The complete proposed system shown in Figure 1 is simulated, the PSIM program is used for simulation with parameters as explained in Table 1. This system is tested with different PV power (1000 W, 2000 W, and 3000 W) by adding PV systems in parallel. For 1 PV string (4 PV panels connected in series), the PV supplied power is 1000 W, the grid current of 2 A with THD% of 4.07% and power factor of 0.998. The three phase grid current is shown in Figure 5 (a), three phase output voltage is shown in Figure 5 (b), and output voltage and grid current of phase a are shown in Figure 5 (c). The output DC current and voltage of boost converter (input to the inverter) of 720V is shown in Figure 6 (a) and boost voltage is shown in Figure 6 (b). The reference and actual Iq currents and I_d current are shown in Figure 7. For 2 PV strings with boost converter for each string (connected in parallel), the PV supplied power is 2000 W, the grid current of 4 A with THD% of 1.85% and power factor of 0.999. The output voltage and grid current of phase a are shown in Figure 8.

Table 1. The parameters of proposed system

| Description	Value
Grid phase voltage	220 V (RMS)
Switching frequency	10 KHz
Inverter side inductor L1	2 mH
Filter capacitor C	1 µF
Grid side inductor L2 + Lg	15 mH
1 PV string voltage	144 V
Light intensity and temperature	1000 W/m², 25 °C
Boosted DC voltage (Inverter DC-link voltage)	720 V
PI parameters of boosted DC voltage loop (k_{pv}, k_{iv})	0.01, 100
PI parameters of PBC controller	8, 800
Damping gains (k1, k2)	0.003333, 6.665

(a)

(b)

(c)
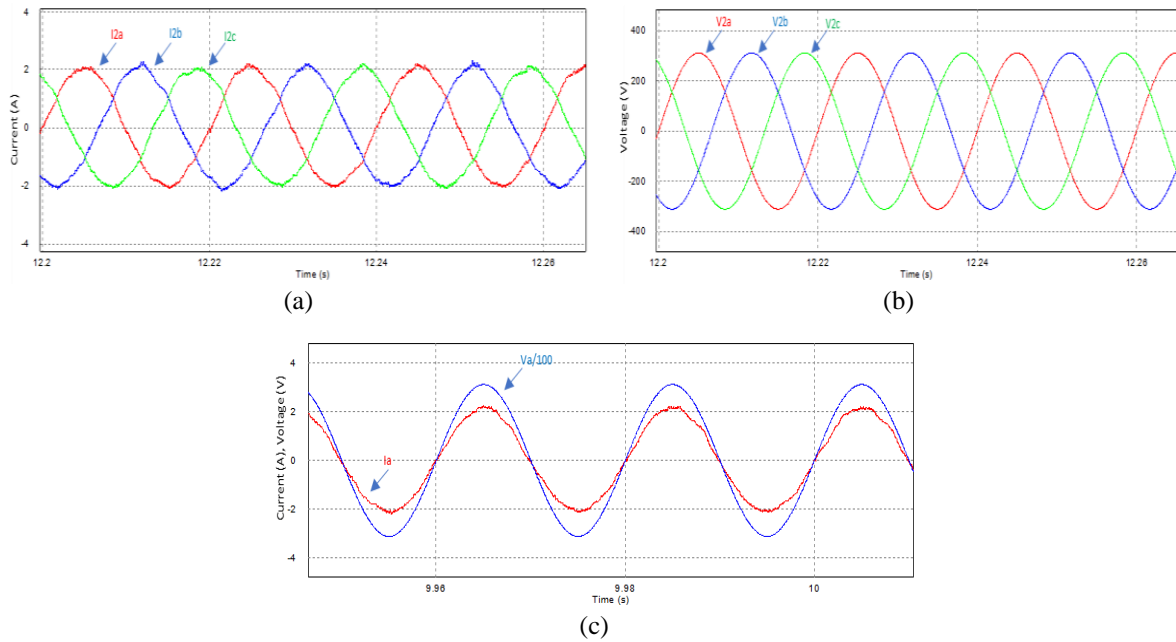
Figure 5. System of 1 PV system (a) three phase of grid current (b) three phase of grid voltage (c) grid current and voltage of phase a
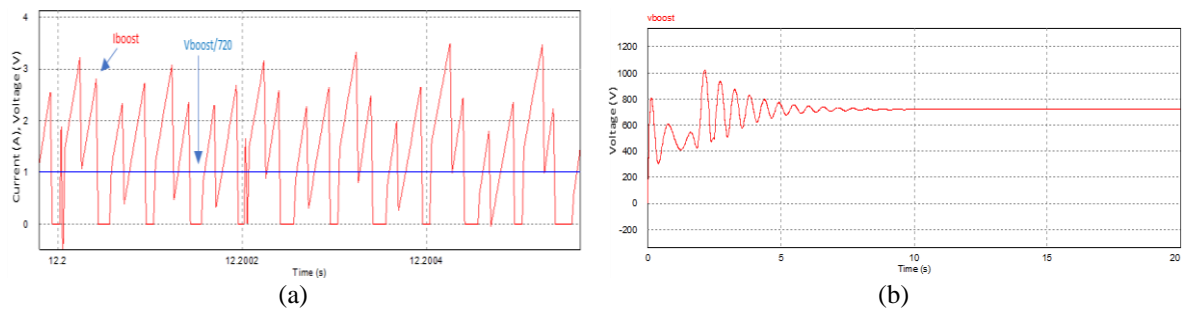

(a)

(b)

Figure 6. System of 1 PV system (a) boost current and voltage (input to the inverter) (b) boost voltage
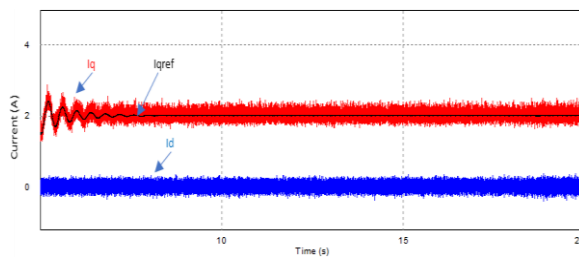

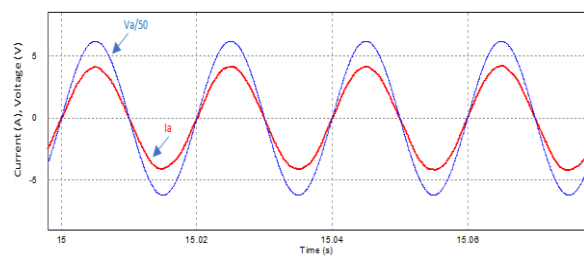Figure 7. I_d and I_q currents for system of 1 PV system

Figure 8. Grid current and voltage of phase a for system of 2 PV systems

For 3 PV strings with boost converter for each string (connected in parallel), the PV supplied power is 3000 W, the grid current of 6A with THD% of 1.38% and power factor of 0.999. The output voltage and current of phase a are shown in Figure 9. The response of the systems above can be summarized as shown in Table 2. To check the robust of the proposed system, there are three tests are applied, the first test is to check the efficiency of the system during weather changes which affect the light intensity, the second test is reduction the inductances of LCL filter, and the last test is to check the system operation with variable grid voltage. A PV system with 2 PV strings is tested in the first test, the light intensity is increased from

800 W/m^2 to 1000 W/m^2 which provides 1600 W PV power (3.2 A grid current) then increased to 2000 W PV power (4 A grid current) at time (10 seconds), the Iq reference of this system is shown in Figure 10 with overshoot of 15% and settled after 1.9 seconds. Boost voltage is shown in Figure 11 with overshoot of 0.48%. The grid current of phase a is shown in Figure 12.
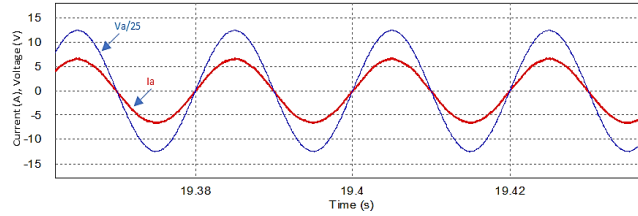

Figure 9. Grid current and voltage of phase a for system of 3 PV systems

Table 2. The results of THD% of grid current and output power factor at different PV power

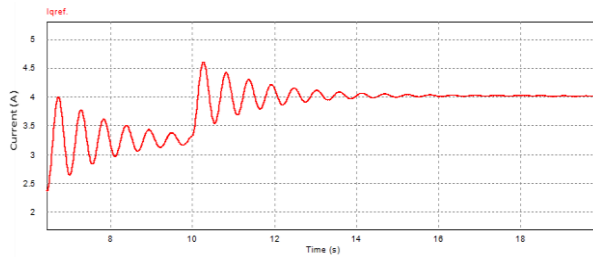| PV system	PV power	Grid current (Amplitude)	System efficiency	THD% of grid current	Power factor
1 PV system	1000 W	2 A	93.15%	4.07%	0.998
2 PV systems	2000 W	4 A	93.24%	1.85%	0.999
3 PV systems	3000 W	6 A	93.24%	1.38%	0.999

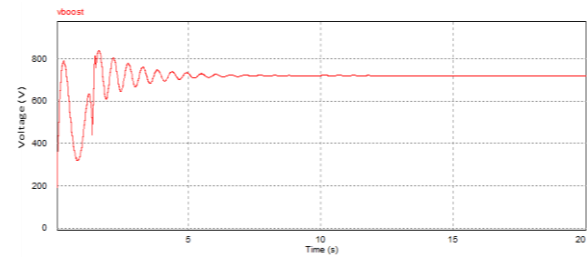Figure 10. The dynamic response of I$_q$ reference current at increasing light intensity

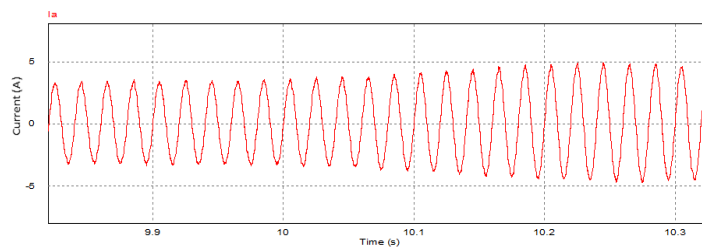Figure 11. The dynamic response of boost voltage at increasing light intensity

Figure 12. The dynamic response of grid current of phase a at increasing light intensity

The same system is tested again with light intensity of 1000 W/m^2 then decreased to 600 W/m^2 which provides 2000 W PV power (4 A grid current) then decreased to 1200 W PV power (2.4 A grid current) at time (14 seconds), the Iq reference of this system is shown in Figure 13 with downshoot of 47% and settled after 2.5 seconds. Boost voltage is shown in Figure 14, the downshoot is 1.25%. The grid current of phase a is shown in Figure 15. The response of the system after applied first test can be summaries as shown in Table 3.

A PV system with 2 PV strings and light intensity of 1000 W/m^2 is tested in this second test, the grid side inductance is reduced from 15 mH to 10 mH, the THD% of grid current is 3% and power factor of 0.999. The output voltage and current of phase a are shown in Figure 16. The same system is tested again with grid side inductance reduced to 6 mH, the THD% of grid current is 4.7% and power factor of 0.998. The output voltage and current of phase a are shown in Figure 17. The same system is tested with inverter side inductance reduced from 2 mH to 1.5 mH, the THD% of grid current is 2.87% and power factor of 0.998. The output voltage and current of phase a are shown in Figure 18. The response of the system under second test can be summarized as shown in Table 4.
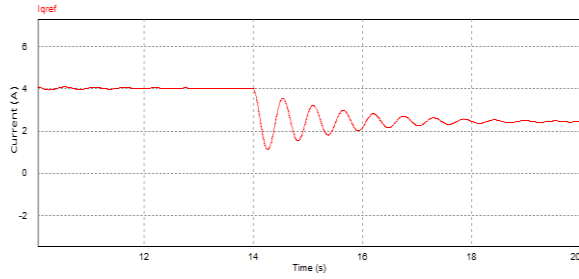
Figure 13. The dynamic response of reference q current at decreasing light intensity
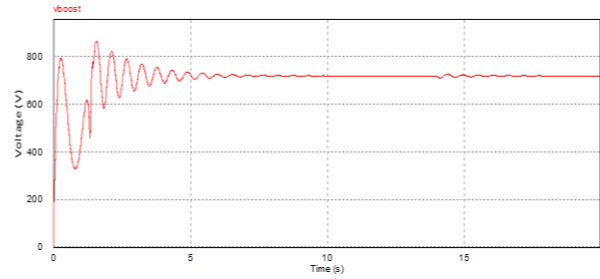

Figure 14. The dynamic response of boost voltage at decreasing light intensity
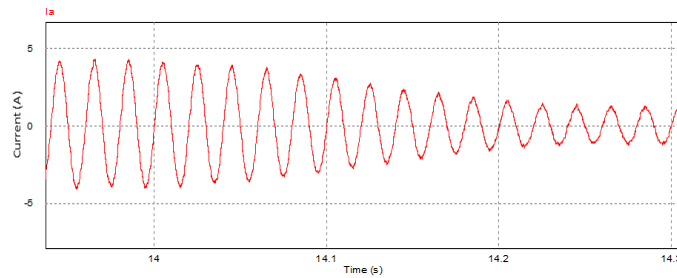

Figure 15. The dynamic response of grid current of phase a at decreasing light intensity

Table 3. the results of shooting% of V boost and Iq and the settling time at difference light intensity

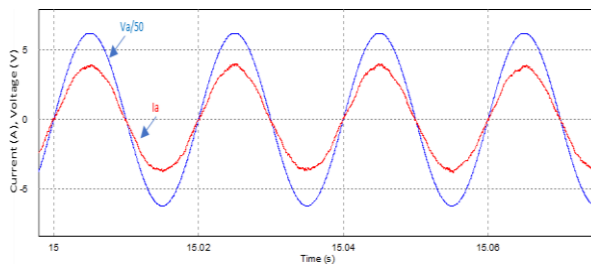| PV system	Light intensity	Grid current (Amplitude)	Shooting% of V boost	Shooting% of Iq reference	Settling time
2 PV systems	800 W/m² to 1000 W/m²	3.2 A to 4 A	0.48%	15% (over)	1.9 seconds
2 PV systems	1000 W/m² to 600 W/m²	4 A to 2.4 A	1.25%	47% (down)	2.4 seconds

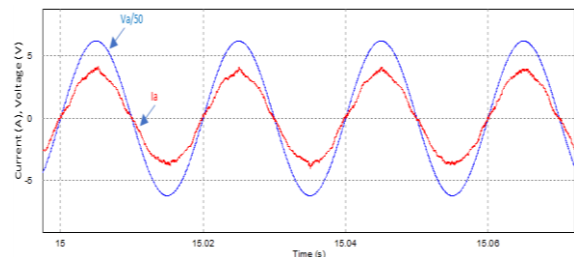Figure 16. Grid current and voltage of phase a at L_1= 2 mH and L_2+L_g= 10 mH

Figure 17. Grid current and voltage of phase a at L_1= 2 mH and L_2+L_g= 6 mH
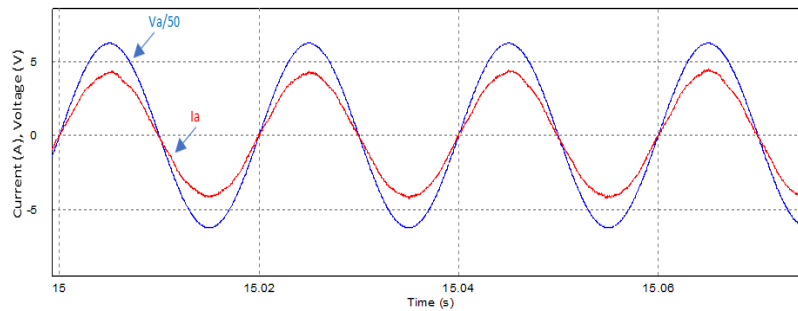

Figure 18. Grid current and voltage of phase a at L_1= 1.5 mH and L_2+L_g= 15 mH

Table 4. The results of THD% of grid current and output power factor at difference filter parameters

PV system	LCL Filter inductances	Grid current (Amplitude)	THD% of grid current	Power factor
2 PV systems	L1= 2mH, L2+Lg=15 mH	4 A	1.85%	0.999
2 PV systems	L1= 2mH, L2+Lg=10 mH	4 A	3%	0.999
2 PV systems	L1= 2mH, L2+Lg=6 mH	4 A	4.7%	0.998
2 PV systems	L1= 1.5mH, L2+Lg=15 mH	4 A	2.87%	0.998

In the third test of a PV system with 2 PV strings, the grid voltage is reduced to 200 V, the PV power is 2000 W, grid current is 4.4 A with THD% of 2.15% and power factor of 0.999. The output voltage and grid current of phase a are shown in Figure 19. The same system is tested again, the grid voltage is increased to 240 V, the PV power is 2000 W, Grid current is 3.4 A with THD% of 2.24% and power factor of 0.999. The output voltage and grid current of phase a are shown in Figure 20. The response of the system under third test can be summarized as shown in Table 5.
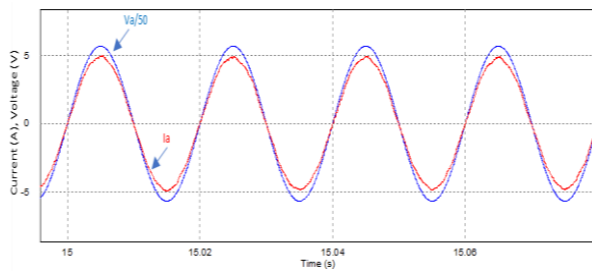

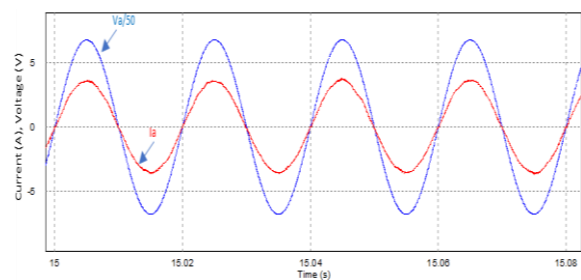Figure 19. Grid current and voltage of phase a at grid voltage of 200 V

Figure 20. Grid current and voltage of phase a at grid voltage of 240 V

Table 5. The results of THD% of grid current and output power factor at difference grid voltage

PV system	Grid voltage (RMS)	Grid current (Amplitude)	THD% of grid current	Power factor
2 PV strings	220 V	4 A	1.85 %	0.999
2 PV strings	200 V	4.4 A	2.15 %	0.999
2 PV strings	240 V	3.4 A	2.24 %	0.999

5. CONCLUSION

In this paper, three-phase photovoltaic grid-connected inverter with an LCL-filter is analyzed and designed. PBC method is suggested in order to find systematic strategy to design the damping factors and to make the system robust against system parameters variation. Based on simulation results, the following aspects can be concluded: i) stable DC-link voltage of inverter against variation in sun light intensity and system parameters variation due to the action of DC voltage loop and PBC controller; ii) the designed PBC controller can maintain the system stable even the parameters of the LCL-filter vary; iii) the system stable against the variation of grid voltage, this due to the effectiveness of PBC controller; iv) the total harmonic distortion of grid current is less than 5% for all tests of proposed grid-connected PV system due to the effectiveness of the LCL- filter and PBC controller; v) the system efficiency is approached to 93.24 % and it is calculated by division the three phase output power on the input PV power.

REFERENCES

[1] C. Poongothai and K. Vasudevan, "Design of LCL Filter for Grid-Interfaced PV System Based on Cost Minimization," *IEEE Transactions on Industry Applications,* vol. 55, no. 1, pp. 584-592, Jan.- Feb. 2019, doi: 10.1109/TIA.2018.2865723.
[2] Y. Guan, Y. Wang, Y. Xie, Y. Liang, A. Lin, and X. Wang, "The dualcurrent control strategy of grid-connected inverter with LCL filter," *IEEE Trans. Power Electron.*, vol. 34, no. 6, pp. 5940–5952, Jun. 2019., doi: 10.1109/TPEL.2018.2869625.
[3] T. Liu, J. Liu, Z. Liu, and Z. Liu, "A study of virtual resistor-based active damping alternatives for LCL resonance in grid-connected voltage source inverters," *IEEE Trans. Power Electron.*, vol. 35, no. 1, pp. 247–262, Jan. 2020, doi: 10.1109/TPEL.2019.2911163.
[4] R. A. Fantino, C. A. Busada, and J. A. Solsona, "Optimum PR control applied to LCL filters with low resonance frequency," *IEEE Trans. Power Electron.,* vol. 33, no. 1, pp. 793–801, Jan. 2018, doi: 10.1109/TPEL.2017.2667409.
[5] A. Kouchaki and M. Nymand, "Analytical Design of Passive LCL Filter for Three-Phase Two-Level Power Factor Correction Rectifiers," *IEEE Trans. Power Electron.*, vol. 33, no. 4, pp. 3012-3022, April 2018, doi: 10.1109/TPEL.2017.2705288.

[6] W. Wu, Y. Liu, Y. He, H. S. H. Chung, M. Liserre, and F. Blaabjerg, "Damping methods for resonances caused by LCL-filter-based current controlled grid-tied power inverters: An overview," *IEEE Trans. Ind. Electron.*, vol. 64, no. 9, pp. 7402–7413, Sep. 2017, doi: 10.1109/TIE.2017.2714143.

[7] Y. He, X. Wang, X. Ruan, D. Pan, X. Xu, and F. Liu, "Capacitor-Current Proportional-Integral Positive Feedback Active Damping for LCL-Type Grid-Connected Inverter to Achieve High Robustness Against Grid Impedance Variation," *IEEE Trans. Power Electron.*, vol. 34, no. 12, pp. 12423-12436, Dec. 2019, doi: 10.1109/TPEL.2019.2906217.

[8] L. Jia, X. Ruan, W. Zhao, Z. Lin, and X. Wang, "An Adaptive Active Damper for Improving the Stability of Grid-Connected Inverters Under Weak Grid," *IEEE Trans. Power Electron.*, vol. 33, no. 11, pp. 95619574, Nov. 2018, doi: 10.1109/TPEL.2018.2793242.

[9] W. Yao, Y. Yang, X. Zhang, F. Blaabjerg, and P. C. Loh, "Design and Analysis of Robust Active Damping for LCL Filters Using Digital Notch Filters," *IEEE Trans. Power Electron.*, vol. 32, no. 3, pp. 2360-2375, March 2017, doi: 10.1109/TPEL.2016.2565598.

[10] M. Ben Sadï-Romdhane, M. W. Naouar, I. Slama-Belkhodja, and E. Monmasson, "Robust Active Damping Methods for LCL Filter-Based Grid-Connected Converters," *IEEE Trans. Power Electron.*, vol. 32, no. 9, pp. 6739-6750, Sept. 2017, doi: 10.1109/TPEL.2016.2626290.

[11] Y. Liu, W. Wu, Y. He, Z. Lin, F. Blaabjerg, and H. S. H. Chung, "An efficient and robust hybrid damper for LCL- or LLCL-based grid-tied inverter with strong grid-side harmonic voltage effect rejection," *IEEE Trans. Ind. Electron.*, vol. 63, no. 2, pp. 926-936, Feb. 2016, doi: 10.1109/TIE.2015.2478738.

[12] J. Ye, A. Shen, Z. Zhang, J. Xu, and F. Wu, "Systematic Design of the Hybrid Damping Method for Three-Phase Inverters With High-Order Filters," *IEEE Trans. Power Electron.*, vol. 33, no. 6, pp. 4944-4956, June 2018, doi: 10.1109/TPEL.2016.2637377.

[13] M. G. Judewicz, S. A. Gonzalez, J. R. Fischer, J. F. Martinez, and D. O. Carrica, "Inverter-side current control of grid-connected voltage source inverters with LCL filter based on generalized predictive control," *IEEE J. Emerg. Sel. Topics Power Electron.*, vol. 6, no. 4, pp. 1732–1743, Dec. 2018, 10.1109/JESTPE.2018.2826365.

[14] S. Bosch, J. Staiger, and H. Steinhart, "Predictive current control for an active power filter with LCL-filter," *IEEE Trans. Ind. Electron.*, vol. 65, no. 6, pp. 4943–4952, Jun. 2018, doi: 10.1109/TIE.2017.2772176.

[15] Y. He, H. S. -H. Chung, C. N. -M. Ho, and W. Wu, "Modified Cascaded Boundary-Deadbeat Control for a Virtually-Grounded Three-Phase Grid-Connected Inverter With LCL Filter," *IEEE Trans. Power Electron.*, vol. 32, no. 10, pp. 8163-8180, Oct. 2017, doi: 10.1109/TPEL.2016.2637078.

[16] X. Xing, C. Zhang, A. Chen, H. Geng, and C. Qin, "Deadbeat Control Strategy for Circulating Current Suppression in Multiparalleled ThreeLevel Inverters," *IEEE Trans. Ind. Electron.*, vol. 65, no. 8, pp. 62396249, Aug. 2018, doi: 10.1109/TIE.2017.2786234.

[17] R. P. Vieira, L. T. Martins, J. R. Massing, and M. Stefanello, "Sliding mode controller in a multiloop framework for a grid-connected VSI with LCL filter," *IEEE Trans. Ind. Electron.*, vol. 65, no. 6, pp. 4714–4723, Jun. 2018, doi: 10.1109/TIE.2017.2772143.

[18] N. Altin, S. Ozdemir, H. Komurcugil, and I. Sefa, "Sliding-mode control in natural frame with reduced number of sensors for three-phase gridtied LCL-interfaced inverters," *IEEE Trans. Ind. Electron.*, vol. 66, no. 4, pp. 2903–2913, Apr. 2019, doi: 10.1109/TIE.2018.2847675.

[19] M. Merai, M. W. Naouar, I. Slama-Belkhodja, and E. Monmasson, "An adaptive PI controller design for DC-link voltage control of single-phase grid-connected converters," *IEEE Trans. Ind. Electron.*, vol. 66, no. 8, pp. 6241–6249, Aug. 2019, doi: 10.1109/TIE.2018.2871796.

[20] Z.-X. Zou, G. Buticchi, and M. Liserre, "Grid identification and adaptive voltage control in a smart transformer-fed grid," *IEEE Trans. Power Electron.*, vol. 34, no. 3, pp. 2327–2338, Mar. 2019, doi: 10.1109/TPEL.2018.2847020.

[21] M. M. Namazi, S. M. S. Nejad, A. Tabesh, A. Rashidi, and M. Liserre, "Passivity-Based Control of Switched Reluctance-Based Wind System Supplying Constant Power Load," *IEEE Trans. Ind. Electron.*, vol. 65, no. 12, pp. 9550-9560, Dec. 2018, doi: 10.1109/TIE.2018.2816008.

[22] J. Min, F. Ma, Q. Xu, Z. He, A. Luo, and A. Spina, "Analysis, Design, and Implementation of Passivity-Based Control for Multilevel Railway Power Conditioner," *IEEE Trans. Ind. Informat.*, vol. 14, no. 2, pp. 415-425, Feb. 2018, doi: 10.1109/TII.2017.2747593.

[23] Z. Liu, Z. Geng, and X. Hu, "An Approach to Suppress Low Frequency Oscillation in the Traction Network of High-Speed Railway Using Passivity-Based Control," *IEEE Trans. Power Syst.*, vol. 33, no. 4, pp. 3909-3918, July 2018, doi: 10.1109/TPWRS.2018.2789450.

[24] Y. Lei, X. Lin, and Y. Zhu, "Passivity-Based Control Strategy for SMES Under an Unbalanced Voltage Condition," *IEEE Access*, vol. 6, pp. 28768-28776, 2018, doi: 10.1109/ACCESS.2018.2831251.

[25] J. Li, X. Lv, B. Zhao, Y. Zhang, Q. Zhang, and J. Wang, "Research on passivity based control strategy of power conversion system used in the energy storage system," *IET Power Electron.*, vol. 12, no. 3, pp. 392–399, Mar. 2019, doi: 10.1049/iet-pel.2018.5620.

[26] Y. Gui, B. Wei, M. Li, J. M. Guerrero, and J. C. Vasquez, "Passivity-based coordinated control for islanded AC microgrid," *Applied Energy*, Vol. 229, pp. 551-561,2018, doi: 10.1016/j.apenergy.2018.07.115.

[27] Y. Chen, M. Wen, E. Lei, X. Yin, J. Lai, and Z. Wang, "Passivity-based control of cascaded multilevel converter based D-STATCOM integrated with distribution transformer," *Electric Power Systems Research*, Vol. 154, pp 1-12, Jan. 2018, doi: 10.1016/j.epsr.2017.08.001.

[28] X. Mu, J. Wang, W. Wu, and F. Blaabjerg, "A modified multifrequency passivity-based control for shunt active power filter with modelparameter-adaptive capability," *IEEE Trans. Ind. Electron.*, vol. 65, no. 1, pp. 760-769, Jan. 2018, doi: 10.1109/TIE.2017.2733428.

[29] J. Wang, X. Mu, and Q. K. Li, "Study of Passivity-based decoupling control of T-NPC PV grid-connected inverter," *IEEE Trans. Ind. Electron.*, vol. 64, no. 9, pp. 7542-7551, Sept. 2017, doi: 10.1109/TIE.2017.2677341.

[30] Y. Jiang, C. Qin, X. Xing, X. Li, and C. Zhang, "A Hybrid PassivityBased Control Strategy for Three-Level T-Type Inverter in LVRT Operation," *IEEE J. of Emerg. Sel. Topics Power Electron.*, vol. 8, no. 4, pp. 4009-4024, Dec. 2020, doi: 10.1109/JESTPE.2019.2928571.

[31] J. Lai, X. Yin, E. Lei, Y. Chen, and X. Yin, "Passivity control based on Euler-Lagrangian model for D-STATCOM with LCL filter," *Proc. of WCICA 2016,* Guilin, 2016, pp. 1561-1565, doi: 10.1109/WCICA.2016.7578498.

[32] J. Lai, X. Yin, Z. Zhang, Z. Wang, Y. Chen, and X. Yin, "System modeling and cascaded passivity based control for distribution transformer integrated with static synchronous compensator," *Int. J. Electr. Power Energy Syst.*, vol. 113, pp. 1035–1046, 2019, doi: 10.1016/j.ijepes.2019.06.015.

[33] J. Zhao, W.Wu, Z. Shuai, A. Luo, H. Sh. Chung, and F. Blaabjerg, "Robust Control Parameters Design of PBC Controller for

LCL-Filtered Grid-Tied Inverter," *IEEE Trans. on Power Electronics,* vol. 35, no. 8, pp. 8102–8115, Aug. 2020, doi: 10.1109/TPEL.2019.2963200.

[34] F. Zheng, W. Wu, B. Chen, and E. Koutroulis, "An Optimized Parameter Design Method for Passivity-Based Control in a LCL-Filtered Grid-Connected Inverter," *IEEE Power & Energy Society Section,* vol. 8, pp. 189878–189890, oct. 2020, doi: 10.1109/ACCESS.2020.3032038.

[35] R. Panigrahi, S. K. Mishra, S. C. Srivastava, A. K. Srivastava, and N. N. Schulz, "Grid Integration of Small-Scale Photovoltaic Systems in Secondary Distribution Network—A Review," *IEEE Transactions on Industry Applications,* vol. 56, no. 3, pp. 3178-3195 May/June 2020, doi: 10.1109/TIA.2020.2979789.

[36] P. Cossoli, M. Cáceres, L. Vera, A. Firman, and A. Busso, "Proportional-Resonant Controller And LCL Filter Design For Single-Phase Grid-Connected PV Micro-Inverters," *IEEE PES Transmission & Distribution Conference and Exhibition - Latin America (T&D-LA),* Oct. 2018, doi: 10.1109/TDC-LA.2018.8511669.

[37] A. Lamichhane, L. Zhou, G. Yao, and M. Luqman, "LCL Filter Based Grid-Connected Photovoltaic System with Battery Energy Storage," *14th IEEE Conference on Industrial Electronics and Applications (ICIEA),* pp. 1569-1574, Sep. 2019, doi: 10.1109/ICIEA.2019.8834271.

[38] J. C. Giacomini, L. Michels, H. Pinheiro, and C. Rech, "Design Methodology of a Passive Damped Modified LCL Filter for Leakage Current Reduction in Grid-connected Transformerless Three-Phase PV Inverters", *IET Renewable Power Generation,* vol. 11, no. 14, pp. 1769-1777, 2017, doi: 10.1049/iet-rpg.2017.0256.

BIOGRAPHIES OF AUTHORS

Zainab Mahmood Abed 🆔 📇 SC Ⓟ was born in 1990. She has received B.Sc. in electrical engineering in 2012, M.Sc. in electrical engineering power and machines in 2017 from Electrical Engineering Department, College of Engineering, Mustansiriyah University, Iraq. From 2012-2017 she was Electrical Engineer in Electrical Engineering Department, College of Engineering, Mustansiriyah University. From 2019 up to now she was assistance lecturer for machine subject in Electrical Engineering Department, College of Engineering, Mustansiriyah University. Her research interests include AC drive systems and grid-connected photovoltaic systems. She can be contacted at email: zainab.mahmood21290@gmail.com.

Turki Kahawish Hassan 🆔 📇 SC Ⓟ was born in 1959. He has received B.Sc. in Electrical Engineering in 1982, M.Sc. in electrical Engineering /Power Electronics Specialisation in 1991 and Ph.D. in electrical engineering power electronics in 2005 from Electrical Engineering Department, College of Engineering, University of Baghdad, Iraq from 1983-2005 he worked in Electrical Engineering Design Centre as designer for DC-AC Converters, and AC-DC Converters. From 2006 up to now He was lecturer for power electronics subject in Electrical Engineering Department, College of Engineering, Mustansiriyah University. He was a professor in 2020. His research interests include modular multilevel converters, high frequency DC-DC converters, AC drive systems and grid-connected photovoltaic systems. He has published 27 journal articles, and 5 international conference articles. He can be contacted at email: thassan2013@yahoo.com.

Kassim Rasheed Hameed 🆔 📇 SC Ⓟ was born in 1960. He has received B.Sc. in Electrical Engineering in 1983, M.Sc. in electrical engineering transformer specialization in 2000 from the University of Technology, Baghdad and Ph.D. in electrical engineering transformer in 2007 from the University of Technology, Baghdad. From 1987 -2007 he worked in the field of manufacturing, Testing and designing electrical transformers at Diyala Company for Transformer Industries in Iraq. He is currently working as an assistant professor in the Department of Electrical Engineering, College of Engineering, Al-Mustansiriya University since 2008. His research interest's High Frequency, Low Frequency Transformer Design and electromagnetic analysis. He has published 8 journal articles. He can be contacted at email: kassim.r.h60@uomustansiriyah.edu.iq.